Soft Matter

PAPER

Aqueous self-assembly of SDS@2β-CD complexes: lamellae and vesicles

Lingxiang Jiang, Yu Peng, Yun Yan and Jianbin Huang*

Cyclodextrin (CD)/surfactant complexes were usually believed to be quite soluble in water and unable to form aggregates because of the hydrophilic outer surface. However, in this work, SDS@2β-CD complex is found to be able to self-assemble into well-defined lamellar structures in concentrated aqueous solution. The lamellae possess unprecedented in-plane solid-crystalline order in addition to classical lamellar liquid-crystalline order. Such a combination in orderliness makes the lamellar phase an intermediate phase between a solid and a liquid crystal. Upon dilution, the lamellae transform to microtubes and then to vesicles. The three classes of SDS@2β-CD aggregates share a consistent building block, the channel-type crystalline bilayer membrane. Moreover, since the outer surface of SDS@2β-CD is hydrophilic, its self-assembly behavior, unlike traditional amphiphilic assembly, does not rely on the hydrophobic effect. Therefore, the present nonamphiphilic self-assembly of SDS@2β-CD is envisioned to open new possibilities for self-assembly chemistry.

Introduction

Cyclodextrins (CDs) are of donut-like structures, formed by oligosaccharides linked in a cycle.[1] The outer surface of CDs is abundant with hydrophilic hydroxyl groups, making CDs water-soluble. The inner cavity is composed of glucoside methylene groups, conferring to the cavity a hydrophobic character. As illustrated in Fig. 1, CDs are able to form host–guest complexes with most surfactants in 1 : 1 and/or 2 : 1 stoichiometries with high binding constants by including surfactant's hydrophobic tails into CD cavities.[2] The resultant complexes are covered on the outer surface with hydrophilic groups which should disfavor
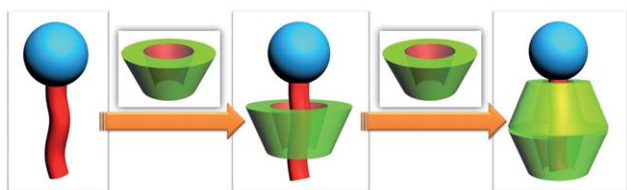

Fig. 1 Schemes of CD/surfactant complexes. For CD/surfactant 1/1 complexes, the mutual direction of CD and surfactant is not certain. The majority of the outer surfaces of 1/1 complexes are hydrophilic. As for CD/surfactant 2/1 complexes, two CD molecules are preferably aligned in a head-to-head fashion to maximize formation of H-bonds. Almost the entire outer surfaces of 2/1 complexes are hydrophilic.

Beijing National Laboratory for Molecular Sciences (BNLMS), State Key Laboratory for Structural Chemistry of Unstable and Stable Species, College of Chemistry and Molecular Engineering, Peking University, Beijing, 100871, P. R. China. E-mail: jbhuang@pku.edu.cn

assembly and render the complexes quite dissolvable in water.[3] This opinion was indeed sufficiently documented in dilute solution, where CDs can break or "weaken" aggregates by removing surfactants from the aggregates. For instance, adding CDs can destroy micelles or air/water interface adsorption layers,[3a] and increase fluidity and permeability of liposomes.[4] However, the anti-assembly nature of CD/surfactant complexes were not tested in concentrated or semi-concentrated solution and scarce work was devoted to study the self-assembly behavior of such complexes.[5]

Recently, nonamphiphilic self-assembly is emerging as a new form of assembly and is drawing increasing attention.[6] Traditionally, self-assembly usually involves amphipilic molecules forming micelles, vesicles, tubes, and lamellae, driven by the hydrophobic effect and mediated by a hydrophobic–hydrophilic balance. In contrast, nonamphiphilic self-assembly does not rely on the hydrophobic effect, for example, assembly of poly-oxometalate macroions, oppositely charged polymers, and non-amphiphilic aromatic organic salts may be governed by electrostatic interactions, including counterion mediation, direct attractions between opposite charges, or salt bridges. Although still in its infancy, nonamphiphilic self-assembly has begun to manifest superiorities in some aspects over its conventional amphiphilic counterpart.[6]

Herein, we report on the nonamphiphilic self-assembly behavior of hydrophilic SDS@2β-CD complexes in water, where SDS is sodium dodecyl sulfate, a common surfactant, β-CD is a CD with 7 oligosaccharides. SDS and β-CD can spontaneously form inclusion complex in a 1 : 2 stoichiometry with a high binding constant. In a most recent publication,[7] we reported annular-ring tubes (*i.e.*, multilamellar tubes) formed in SDS@2β-CD aqueous solution from *C* (total mass concentration of SDS

and β-CD) = 6 to 25 wt%. In this work, the studied concentration range is extended to 25 to 50 wt%, where lamellar structures are found, and to 4 to 6 wt%, in which vesicles were revealed. Moreover, the building block of these aggregates is identified as a channel-type bilayer membrane of SDS@2β-CD.

Experimental section

Materials

Sodium dodecyl sulfate (SDS, 99%) was purchased from Acros Organics Co. and used as received. The purity of SDS was testified by the absence of minimum in its surface tension curve. β-Cyclodextrin (β-CD) was purchased from Sinopharm Chemical Reagent Co. with a water content of 14%. Water (H_2O) was redistilled from potassium permanganate.

Freeze-fracture transmission electron microscopy (FF-TEM)

Before the freezing procedure, samples were always incubated at 25 °C for more than 2 h. In the freezing procedure, a small amount of a sample was placed on a 0.1 mm thick copper disk and then covered with a second copper disk. The sample-loaded copper sandwich was frozen by plunging this sandwich into liquid propane which was cooled by liquid nitrogen. Aggregate structures were believed to be preserved and "solidified" by this procedure. Fracturing and replication were carried out in a freeze-fracture apparatus (BalzersBAF400, Germany) at −140 °C. Pt/C was deposited at an angle of 45° to shadow the replicas, and C was deposited at an angle of 90° to consolidate the replicas. The resulting replicas were examined in a JEM-100CX electron microscope. TEM micrographs were obtained with a JEM-100CX II transmission electron microscope (working voltage of 80–100 kV).

Confocal laser scanning microscopy (CLSM)

Vesicular samples were stained by Nile red in the following way. 15 µL stock solution of Nile red in acetone (1 mg mL^{-1}) was added to a test tube, followed by volatilization of the acetone. A desired amount of SDS@2β-CD aqueous solution was then added to the tube. The stained samples were allowed for equilibrium for 24 h. A drop (about 10 µL) of the samples was sealed between two slides, ready for CLSM observation. A TCS-sp inverted confocal laser scanning microscope (Leica, Germany) was used to conduct experiments in florescence and differential interference contrast (DIC) modes.

Atomic force microscopy (AFM)

AFM measurements were conducted by Nanoscope IIIa (Digital Instruments Inc., USA) in tapping mode under ambient conditions.

Small- and wide-angle X-ray scattering (SAXS and WAXS)

Measurements were performed by a highflux SAXSess (Anton-Paar, Austria, Cu-Kα, λ = 0.154 nm), equipped with a Kratky block-collimation system and an imaging plate (IP) as the detector. Both SAXS and WAXS scattering profiles can be simultaneously recorded. The scattering peak positions were calibrated with silicon powder for the wide-angle region and silver behenate for the small-angle region. A temperature control unit (Anton-Paar TCS-120) in conjunction with the SAXSess was utilized to control the temperature at 25 °C. Samples were loaded into a quartz capillary with a diameter of 1 mm. An exposure time of 15 min was found to be long enough to give a good signal-to-noise ratio. The scattering curve of pure water filled in the same capillary was recorded as the background.

Results and discussion

For sample preparation, desired amounts of β-CD, SDS, and water were weighed into tubes to give a constant β-CD/SDS molar ratio of 2 : 1 and different total mass concentration of β-CD and SDS, C; the samples were heated to obtain transparent and isotropic solutions, where SDS@2β-CD is formed as the major component; the solutions were then thermostatically incubated at 25 °C (for at least 48 h) to allow SDS@2β-CD to form aggregates. The aggregates are considered to be spontaneously formed because no energy input (such as sonication or extrusion) is involved. According to aggregate morphologies, the whole studied concentration range is divided into three regions, that is, region I, II, and III for lamellae, microtubes, and vesicles, respectively. The solutions and aggregates therein are stable for months as verified by repeatable results after a long incubation time.

Lamellar phase

In region I (C = 50–25 wt%), the SDS@2β-CD solutions are semi-transparent as observed by the naked eye and display strong static birefringence under crossed polarizer. The birefringence is an indication of an anisotropic phase. Typical pictures of a 30 wt% sample are shown in Fig. 2a. Microstructures in these solutions were investigated by freeze-fracture transmission electron microscopy (FF-TEM), a technique that allows unveiling inner structures. In this technique, the samples were vitrified to preserve the original structures and then fractured to expose cross sections of the structures; replicas of the fracture surface were shadowed by platinum and observed under TEM (for details, please see the Experimental Section). As shown in Fig. 2b and 2c for the 30 wt% sample, the images are full of numerous parallel lines with a uniform interval, typical for cross sections of lamellar structures.

Meanwhile, small-angle X-ray scattering (SAXS) profiles of 30, 40, and 50 wt% samples (Fig. 3a) are characterized by a set of
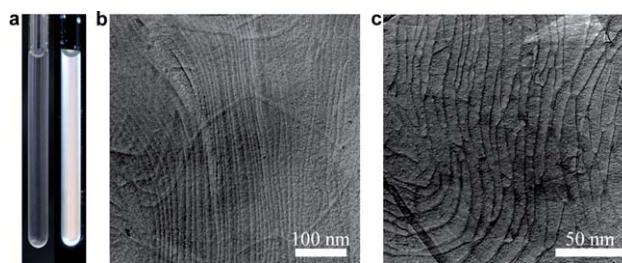

Fig. 2 a), macroscopic photos of the 30 wt% SDS@2β-CD sample without (left) or with (right) crossed polarizer. b) and c), FF-TEM micrographs of the 30 wt% SDS@2β-CD sample.

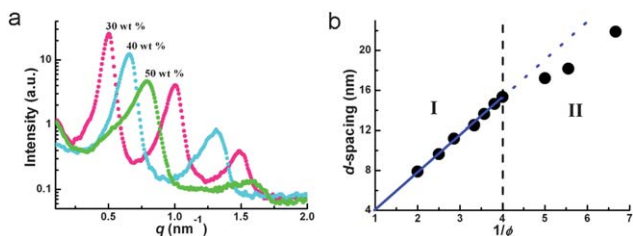**Fig. 3** a) SAXS profiles for the 50, 40, and 30 wt% SDS@2β-CD samples. b) d-spacing versus 1/φ in region I and II.

Bragg peaks with regular spacings. The peak positions can be clearly indexed 1, 2, and 3, consolidating the FF-TEM results and confirming the existence of lamellar structures. Moreover, further analysis of SAXS data can clarify whether the lamellar structures fill the entire solution (i.e., pure lamellar phase) or if the lamellar structures coexist with other phases,[8] such as dilute solution phase. By subjecting the peak position of the first harmonic q_1 to the equation $d = 2\pi/q_1$, one obtains the repeat distance d (or d-spacing). In this case, d is the sum of the thickness of the SDS@2β-CD membrane t and that of the water layer. Fig. 3b shows an inversely linear dependence of the d-spacing on the volume fraction of the membranes φ ($d \propto 1/\varphi$) in region I. Such a relationship of $d \propto 1/\varphi$ suggests that this anisotropic phase is a pure lamellar phase.[8] Furthermore, membrane thickness t can be determined. It has been well documented that in pure lamellar phase the lamellae will linearly swell upon dilution as governed by the classical relationship, $d = t/\varphi$, where t keeps constant on dilution. Accordingly, t of the present membrane is the slope of the fitting line in Fig. 3b, which gives $t = 3.9$ nm. This value is approximately double the length of SDS@2β-CD (~2 nm, by molecular modeling), signaling a bilayer structure without significant tilting or interpenetration for the membranes.

Fine structures of the lamellar membranes are probed by wide-angle X-ray scattering (WAXS) analyses. Representative WAXS patterns of the 30 and 50wt% samples are plotted in Fig. 4. The WAXS patterns are dominated by many sharp diffraction peaks, which will be ascribed to in-plane crystalline structures. Although these WAXS patterns do not allow resolution the structures in the atomic scale, insights into the structures can be gained by comparing the patterns with those of well-documented analogues. Crystalline structures of β-CD and its inclusion complexes were mainly classified into cage-type and channel-type ones (see the inserted sketches in Fig. 4).[9] Cage-type compounds (e.g., β-CD) display major peaks at 6.8, 9.1, 9.4, and 12.8 nm⁻¹; channel-type compounds (e.g., the inclusion complexes of β-CD with poly(propy1ene glycol)[10] or trans-cinnamic acid (tCA)[11]) exhibit characteristic peaks at 8.2 and 12.4 nm⁻¹ as highlighted by cyan dotted lines. Comparison of the patterns in Fig. 4 clearly reveals a channel-type structure for the present membranes. In addition, for channel-type compounds, β-CD molecules will be aligned in a head-to-head fashion along the "channels" to maximize the formation of H-bonds. In the light of the WAXS results and membrane thickness ~4 nm, we propose a channel-type crystalline bilayer architecture for the SDS@2β-CD membranes as illustrated in Fig. 8c.

The present lamellar phase features unprecedented crystalline order in the two in-plane dimensions in addition to classical
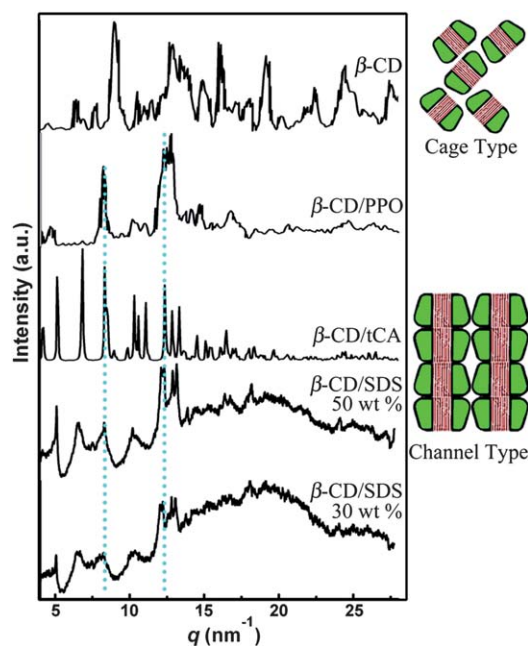

Fig. 4 WAXS patterns of β-CD powders (cage-type), β-CD/PPO and β-CD/tCA powders (channel-type), and SDS@2β-CD solutions (50 and 30 wt%).

lamellar order in the normal-to-plane dimension. The unique combination of lamellar and crystalline order differentiates the lamellae from traditional lipid lamellae (less-ordered in a fluid state or ill-ordered in a gel state) and 2-D interfacial crystals or arrays[12] (confined to interface rather than filled the whole bulk solution). It is well-known that liquid crystals are substances that blend the structures and properties of liquids and solids.[13] Likewise, this lamellar phase appears to be an intermediate phase between a liquid crystal and a solid because it is of liquid-crystalline order in one dimension and solid-crystalline order in the other two dimensions.

Tubular phase

In region II ($C = 25$–6 wt%), unique multilamellar microtubes were identified. The tubes are consist of a set of coaxial, equally spaced, hollow cylinders, resembling the annular rings of trees (thus termed as "annular ring" microtubes). The building block of those tubes was found identical to that of the lamellae, i.e., the channel-type bilayer membrane yet with much weaker in-plane crystalline order. This phase was investigated in details in our previous work.

Vesicular phase

In region III ($C = 6$–4 wt%), the SDS@2β-CD solutions are of a bluish appearance and have a water-like viscosity, both of which parallel those of typical lipid vesicular solutions. For the 5 wt% system, the FF-TEM micrographs (Fig. 5a and 5b) demonstrate two coexisting populations of spherical structures with diameters of ~700 nm and ~100 nm, respectively. Both the large and small spherical structures turn out to be hollow vesicles rather than solid spheres (see the AFM results below). Most of
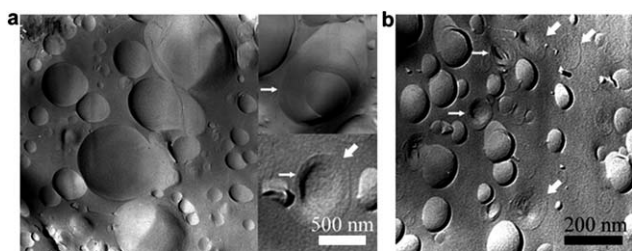
Fig. 5 Images acquired by FF-TEM for vesicles in 5 wt% SDS@2β-CD solution.

the vesicles appear as convex or concave surfaces, corresponding to the fracture surface being propagated along the vesicular membranes; a few circles can be found (see the big arrows in Fig. 5a and 5b), in line with the cross-membrane fracture surface. The micrographs present prevailingly plenty of unilamellar vesicles as well as several bilamellar vesicles (denoted by small arrows in Fig. 5a and 5b). The lack of multilamellar vesicles is in agreement with the disappearance of diffraction peaks in the SAXS profile. After staining with Nile Red (NR), the samples were observed in a hydrated state by confocal laser scanning microscopy (CLSM) in fluorescence mode. It was reported that NR can partly insert into β-CD cavities in β-CD aqueous solution,[14] NR is thus anticipated to positively stain the aggregates in this case. As expected, the formation of the large vesicles is supported by the prevalence of spheres with comparable diameters in CLSM images, as shown in Fig. 6a. Similar spherical structures are observed by CLSM in differential interference contrast (DIC) mode (Fig. 6b, not stained by NR), which rules out the possibility that the added trace amount of NR will affect the SDS@2β-CD aggregates. But the small vesicles are invisible to optical microscopy due to the resolution limitation.

The 5 wt% sample was further studied by atomic force microscopy (AFM) in a dehydrated state, in which two populations of disks are found, as reported in Fig. 7a and 7b. These disks display diameters (matching those of the large and small vesicles, respectively) far larger than their heights; it is noteworthy that many of the large disks are actually "donutlike" structures with their centers lower than their edges (see the inserted 3-D height plot in Fig. 7c). This evidence implies that the spheres observed by CLSM or FF-TEM are water-filled vesicles that will collapse into the dehydrated donuts or disks detected by AFM. Fig. 7c shows a sectional height profile for a donut, where
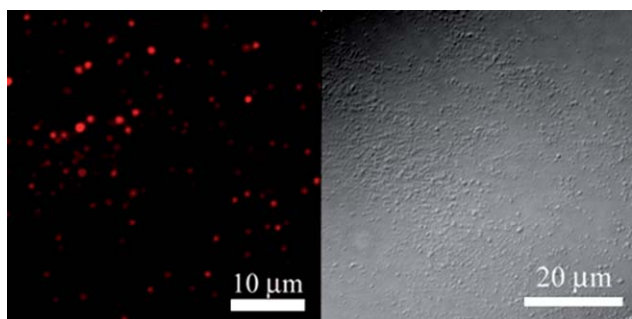

Fig. 6 Images acquired by CLSM in fluorescence (left) and DIC (right) modes for vesicles in 5 wt% SDS@2β-CD solution.

the lowest height in the crater part is ∼8 nm. This height is consistent with the thickness of two closely stacked bilayer membranes (see the inserted cartoon in Fig. 7c). The WAXS pattern of this sample, however, gives no recognizable diffraction peak. The thickness and WAXS results suggest that the vesicular membranes have basically a bilayer structure (Fig. 8c) but that the in-plane crystalline order vanishes.

Structural evolution from lamellae *via* microtubes to vesicles

Taken together, the results are clearly indicative of the self-assembly behavior of SDS@2β-CD in aqueous solution. The aggregates transform, upon dilution, from lamellae *via* microtubes to vesicles, all of which share a consistent building block, the bilayer membrane (Fig. 8c). The connection between the membrane and the demonstrated aggregate morphologies is reported in Fig. 8: the membranes will laterally expand into the lamellar structures in region I, extend in one direction and scroll up in the perpendicular direction to form the annual-ring microtubes in region II, and close up along two in-plane axis to generate vesicles in region III. In addition, lamella–microtube and microtube–vesicle coexistence are respectively observed in solutions with C near boundaries of region I/II and II/III. Fig. 9 left and 9 right show CLSM pictures of two samples with $C = 20$ wt% and 7 wt%, respectively, as stained by NR. In Fig. 9 left, there are several pairs of red-fluorescent parallel lines separated by a non-fluorescent center, consistent with the longitudinal-sectional view of hollow tubular structures with their walls being positively stained. Besides, there are some red plates in line with lamellar structure. In Fig. 9 right, plenty of microtubes and a few spherical vesicles can be found. The coexistence of different aggregates indicates that the aggregate transitions are second-order phase transitions.

Conclusions and perspective

In conclusion, we have archived a novel kind of nonamphiphilic self-assembly in aqueous solutions of SDS@2β-CD complexes. The aggregates transform upon dilution from lamellae *via* microtubes to vesicles with a consistent building block, the channel-type crystalline bilayer membrane. Such a building block can laterally expand into infinite two-dimensional (2-D) lamellar structures at high concentrations, disconnect and scroll up along one axis into 1-D multilamellar microtubes upon dilution, and further close along another axis into dispersed vesicles upon further dilution. Among the aggregates, the lamellae are an example of in-plane crystalline architecture in addition to classical out-of-plane liquid-crystalline order. The present lamellar structure can be regard as an intermediate phase between a liquid crystal and a solid. This intermediate phase might open new possibilities for materials in mechanical, optical, or electrical properties. Furthermore, the hydrophilic outer surface of SDS@2β-CD rules out the possibility that its self-assembly is driven by hydrophobic effect. Alternatively, it may be driven by H-bonds and mediated by electrostatic interactions, as proposed in our previous publication.

Study on the present nonamphiphilic SDS@2β-CD self-assembly is, however, still in its infancy, which leaves some critical issues not being fully addressed. For example, although
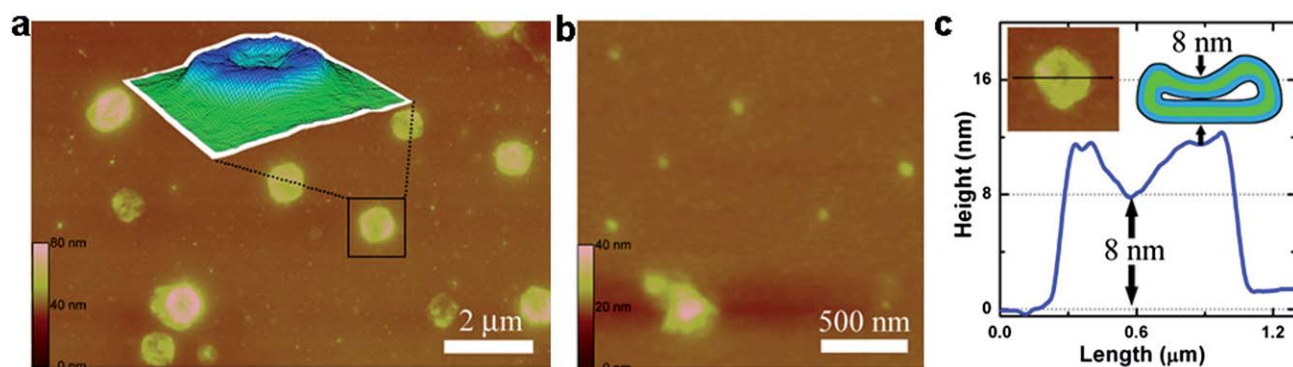
Fig. 7 a) and b) Images acquired by AFM for vesicles in 5 wt% SDS@2β-CD solution. c) Sectional height profile of a collapsed unilamellar vesicle.
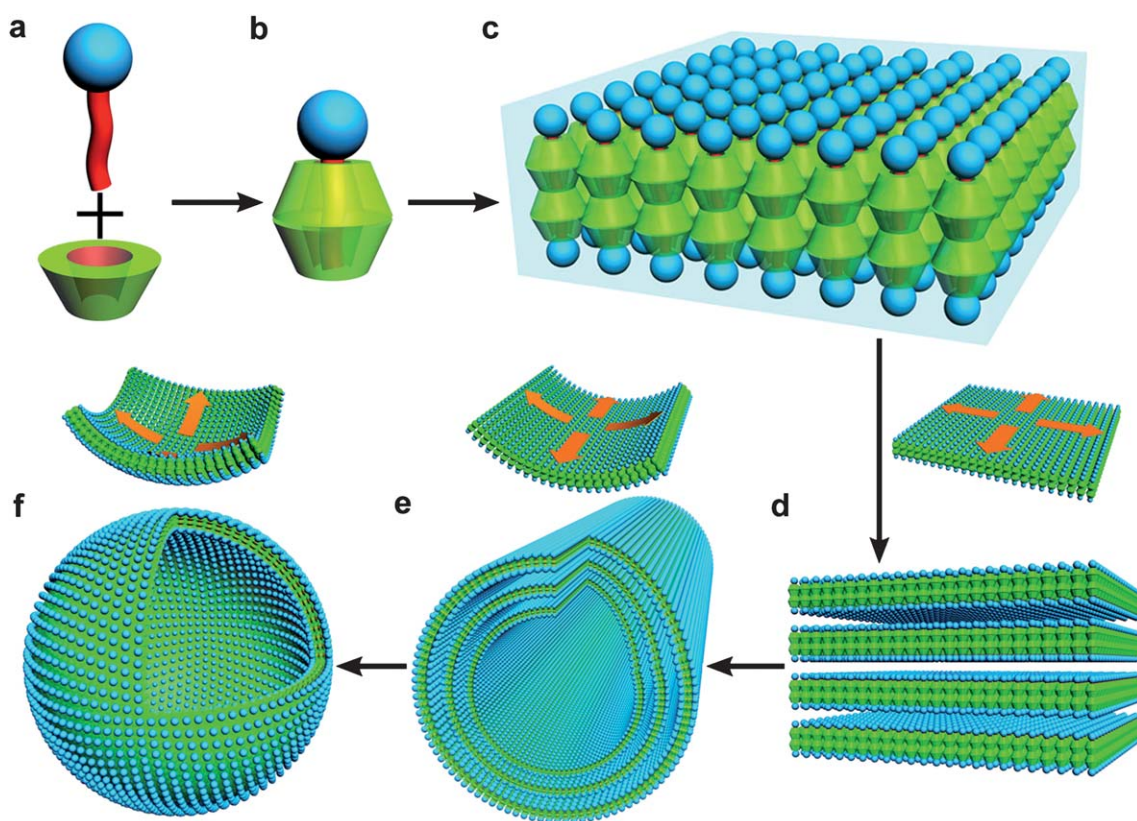

Fig. 8 Schematic self-assembly behavior of SDS@2β-CD. a) SDS and β-CD monomers. b) SDS@2β-CD complex. c) The SDS@2β-CD bilayer membrane with a channel-type crystalline structure. d), e) and f) The aggregates transform upon dilution from lamellae *via* microtubes to vesicles.
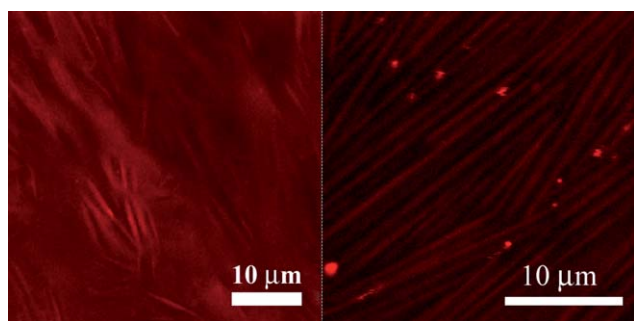

Fig. 9 Left, CLSM image for the 20 wt% sample, showing the coexistence of lamellae and microtubes. Right, CLSM image for the 7 wt% sample, showing the coexistence of microtubes and vesicles.

H-bonds were considered to be the main driving force (supported by indirect evidence), direct and strong evidence is required to draw an unambiguous conclusion. Another issue is why would the SDS@2β-CD bilayers fold up into tubes and vesicles upon dilution just like typical lipid bilayers do. Lipid bilayers tend to fold up to minimize unfavorable contacts between water and the hydrophobic tails at the ends of a bilayer sheet. On the other hand, SDS@2β-CD bilayers also tend to fold up and eliminate edges of a bilayer sheet, as we speculated, to maximizing lateral H-bonding network between SDS@2β-CD complexes. Moreover, other details such as the structure in the open ends of tubes are quite intriguing. Further study on the SDS@2β-CD system would certainly unveil the system itself and will also shed more light on self-assembly chemistry.

Notes and references

1 (*a*) A. Harada, J. Li and M. Kamachi, *Nature*, 1992, **356**, 325–327; (*b*) M. V. Rekharsky and Y. Inoue, *Chem. Rev.*, 1998, **98**, 1875–1918.
2 (*a*) A. B. Dorrego, L. Garcia-Rio, P. Herves, J. R. Leis, J. C. Mejuto and J. Perez-Juste, *Angew. Chem. Int. Ed.*, 2000, **39**, 2945–2948; (*b*) J. W. Park and H. J. Song, *J. Phys. Chem.*, 1989, **93**, 6454–6458; (*c*) U. R. Dharmawardana, S. D. Christian, E. E. Tucker, R. W. Taylor and J. F. Scamehorn, *Langmuir*, 1993, **9**, 2258–2263; (*d*) L. X. Jiang, M. L. Deng, Y. L. Wang, Y. Yan and J. B. Huang, *J. Phys. Chem. B*, 2009, **113**, 7498–7504; (*e*) L. X. Jiang, C. F. Yu, M. L. Deng, C. W. Jin, Y. L. Wang, Y. Yan and J. B. Huang, *J. Phys. Chem. B*, 2010, **114**, 2165–2174.
3 (*a*) W. Saenger and A. Muller-Fahrnow, *Angew. Chem., Int. Ed. Engl.*, 1988, **27**, 393–395; (*b*) E. Junquera, G. Tardajos and E. Aicart, *Langmuir*, 1993, **9**, 1213–1217; (*c*) H. Mwakibete, R. Cristantino, D. M. Bloor, E. Wyn-Jones and J. F. Holzwarth, *Langmuir*, 1995, **11**, 57–62.
4 (*a*) J. Nishijo, S. Shiota, K. Mazima, Y. Inoue, H. Mizuno and J. Yoshida, *Chem. Pharm. Bull.*, 2000, **48**, 48–52; (*b*) G. Puglisi, M. Fresta and C. A. Ventura, *J. Colloid Interface Sci.*, 1996, **180**, 542–547.
5 J. Haller and U. Kaatze, *J. Phys. Chem. B*, 2009, **113**, 1940–1947.
6 (*a*) T. Liu, E. Diemann, H. Li, A. W. Dress and A. Muller, *Nature*, 2003, **426**, 59–62; (*b*) D. Li, J. Zhang, K. Landskron and T. Liu, *J. Am. Chem. Soc.*, 2008, **130**, 4226–4227; (*c*) I. K. Voets, A. de Keizer and M. A. Cohen Stuart, *Adv. Colloid Interface Sci.*, 2009, **147–148**, 300–318; (*d*) A. Harada and K. Kataoka, *Science*, 1999, **283**, 65–67; (*e*) L. Wu, J. Lal, K. A. Simon, E. A. Burton and Y.-Y. Luk, *J. Am. Chem. Soc.*, 2009, **131**, 7430–7443.
7 L. X. Jiang, Y. Peng, Y. Yan, M. L. Deng, Y. L. Wang and J. B. Huang, *Soft Matter*, 2010, **6**, 1731–1736.
8 (*a*) M. Dubois and T. Zemb, *Langmuir*, 1991, **7**, 1352–1360; (*b*) H. E. Warriner, S. L. Keller, S. H. J. Idziak, N. L. Slack, P. Davidson, J. A. Zasadzinski and C. R. Safinya, *Biophys. J.*, 1998, **75**, 272–293.
9 W. Saenger, J. Jacob, K. Gessler, T. Steiner, D. Hoffmann, H. Sanbe, K. Koizumi, S. M. Smith and T. Takaha, *Chem. Rev.*, 1998, **98**, 1787–1802.
10 A. Harada, M. Okada, J. Li and M. Kamachi, *Macromolecules*, 1995, **28**, 8406–8411.
11 A. Kokkinou, S. Makedonopoulou and D. Mentzafos, *Carbohydr. Res.*, 2000, **328**, 135–140.
12 H. Zepik, E. Shavit, M. Tang, T. R. Jensen, K. Kjaer, G. Bolbach, L. Leiserowitz, I. Weissbuch and M. Lahav, *Science*, 2002, **295**, 1266–1269.
13 E. B. Priestley. *Introduction to Liquid Crystals*, Plenum Press, New York, 1975.
14 (*a*) B. D. Wagner, N. S. Stojanovic, G. Leclair and C. K. Jankowski, *J. Incl. Phenom. Macro. Chem.*, 2003, **45**, 275–283; (*b*) P. Hazra, D. Chakrabarty, A. Chakraborty and N. Sarkar, *Chem. Phys. Lett.*, 2004, **388**, 150–157.